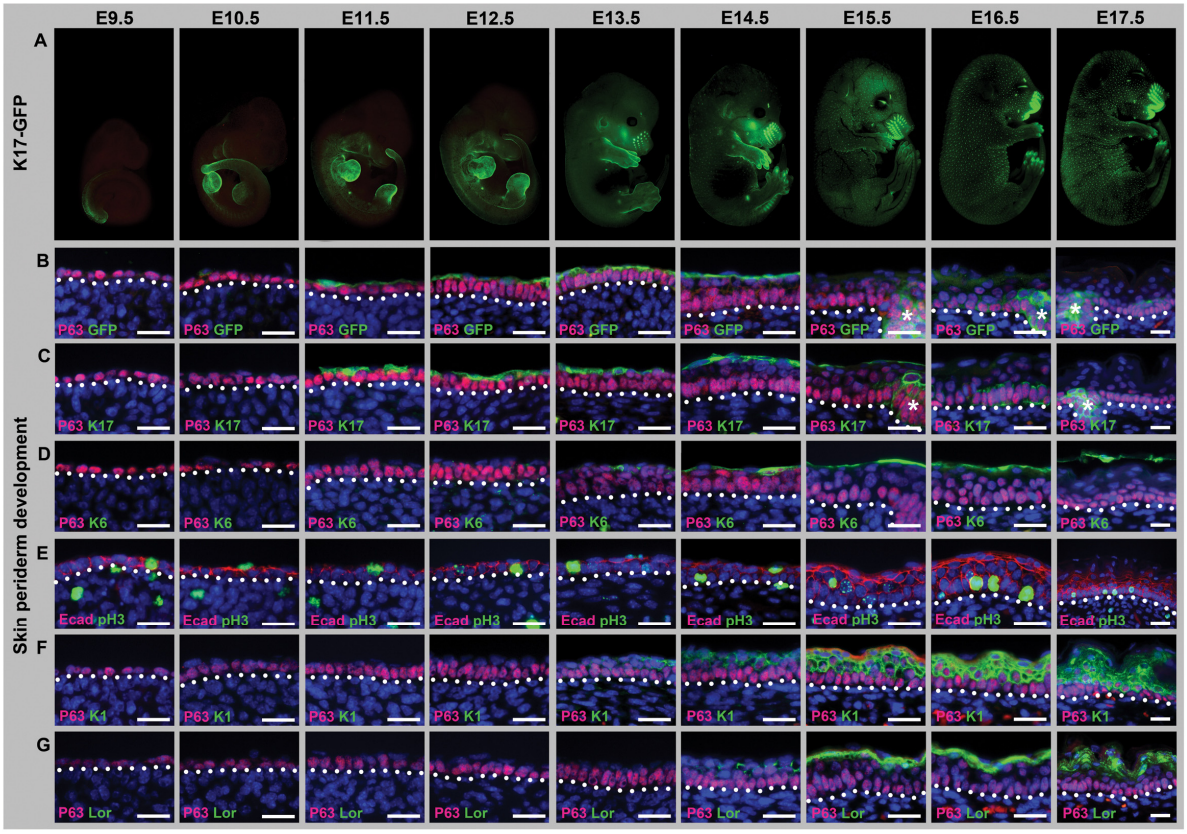

Supplemental Figure 1. Epidermal periderm development during embryogenesis. (**A**) Fluorescence visualization of [*mK17* 5']-GFP transgenic mice reveals that periderm (green) forms in a distinct pattern. Periderm appears over the developing tail at E9.5 and limb buds at E10.5 before spreading in a wave over the trunk and head. Placodes and hair follicles on the trunk become GFP-positive from E14.5 onwards. (**B**) Dual immunofluorescence for p63 (red) and GFP (green) reveal GFP-positive periderm cells above a single layer of p63-positive basal cells from E11.5. As the epidermis differentiates, GFP expression persists until E15.5 when it is down-regulated in periderm and subsequently up-regulated in placodes and hair follicles (asterisked). (**C**) Keratin 17 (green) immunofluorescence faithfully reproduces the GFP expression pattern. (**D**) Keratin 6 (green) is expressed exclusively in periderm from E13.5 onwards and is present in shedding periderm at E17.5. (**E)** Dual immunofluorescence for phospho-histone H3 (green) to label mitotic cells and E-cadherin (red) to highlight cell layers, demonstrates the periderm layer is proliferative from E10.5 - E14.5. (**F** and **G**) Markers of terminal differentiation, keratin 1 (**F**; green) and loricrin (**G**, green) are expressed in stratifying epithelial layers below the periderm from E13.5 and E14.5, respectively. Dotted lines indicate the position of the basement membrane. Scale bars: 25 µm.

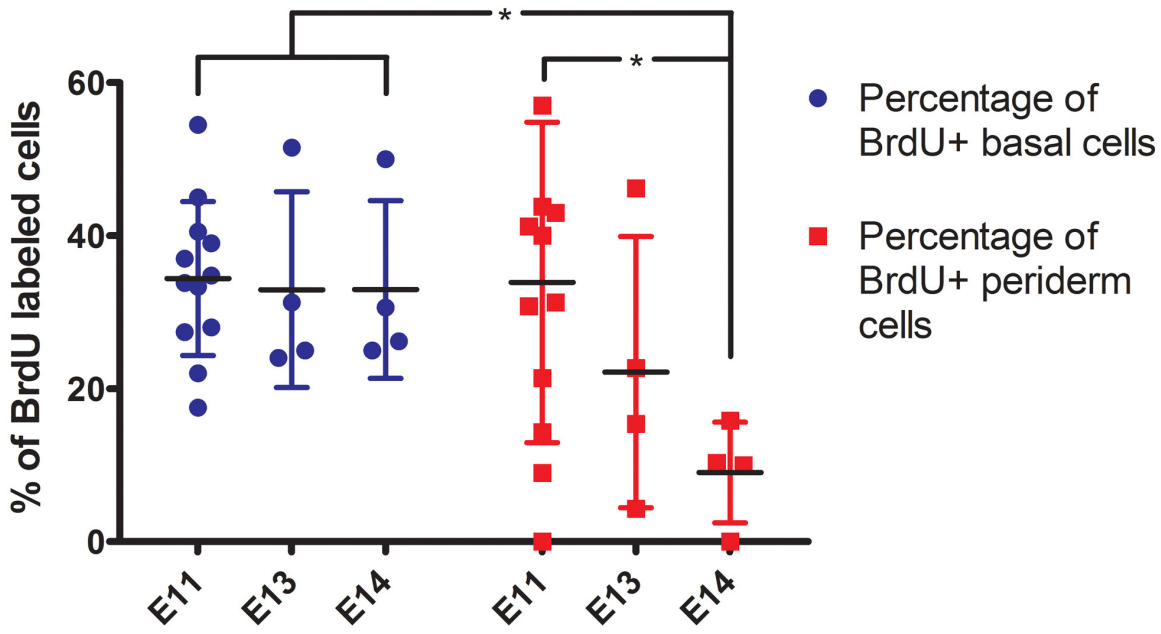

Supplemental Figure 2. Quantification of BrdU incorporation during early epidermal development. Dot plot demonstrating the number of BrdU-labelled basal (blue) or periderm (red) cells as a percentage of the total number of cells from each respective layer within a single field of view at the ages indicated. The number of fields of view counted from at least two different mice at each age are: E11: n=12, E13: n=4, E14: n=4. Statistical significance was calculated using a Student's t-test (* = $p < 0.05$).

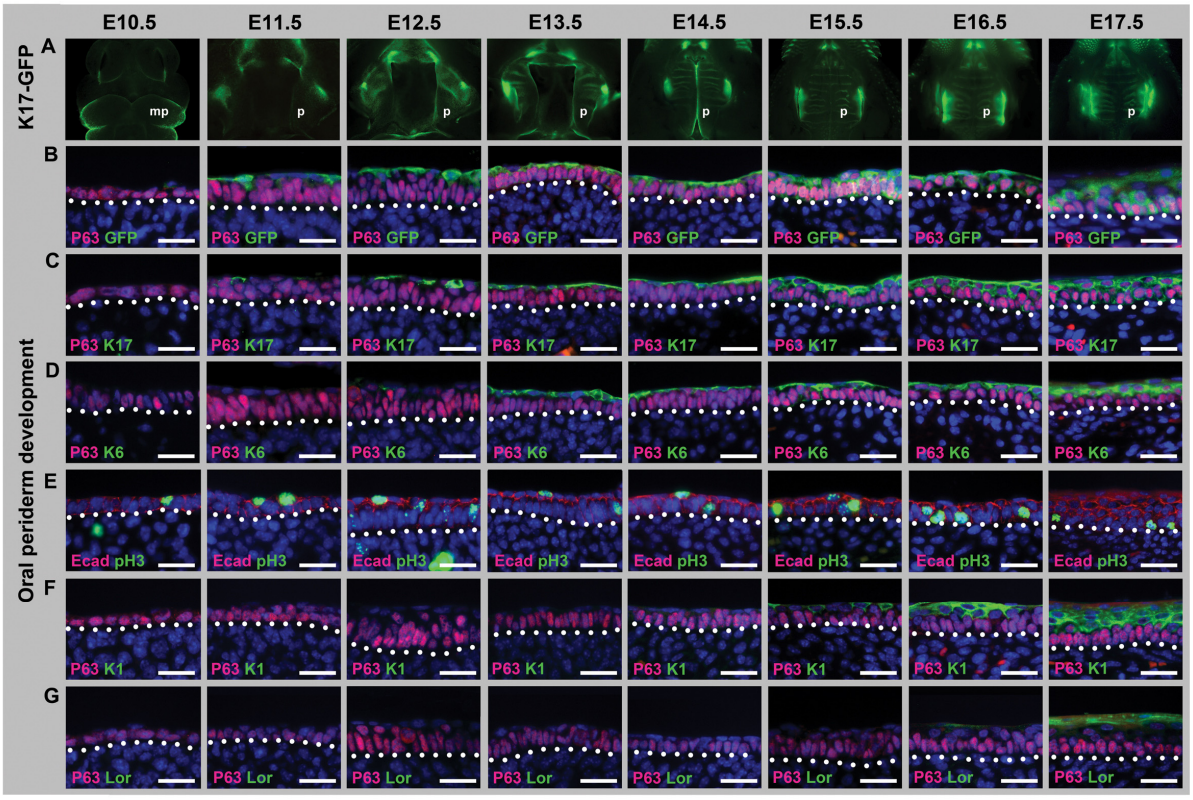

Supplemental Figure 3. Oral periderm development during palatogenesis. (**A**) Fluorescence visualization of developing facial processes or palatal shelves of [*mK17* 5']-GFP transgenic mice reveals that periderm (green) forms in a distinct pattern. Periderm appears over the facial processes at E10.5 and maxillary processes at E11.5 before covering the palatal shelves. Developing tooth-germs and rugae are also GFP-positive from E12.5 onwards. (**B**) Dual immunofluorescence for p63 (red) and GFP (green) reveals GFP-positive periderm cells above a single layer of p63-positive basal cells at E11.5. As palatal epithelium differentiates, GFP expression is expanded to label all cell layers from E15.5 onwards. (**C**) Keratin 17 (green) immunofluorescence faithfully reproduces the GFP expression pattern. (**D**) Keratin 6 (green) is expressed in periderm from E13.5 onwards (**E)** Dual immunofluorescence for phospho-histone H3 (green; to label mitotic cells) and E-cadherin (red; to highlight cell layers) demonstrates the periderm layer is proliferative from E11.5 - E15.5. (**F** and **G**) Late markers of terminal differentiation, keratin 1 (**F**; green) and loricrin (**G**, green) are expressed in differentiating epithelial layers from E15.5 and E16.5, respectively. Dotted lines indicate the position of the basement membrane. mp, maxillary process; p, palate. Scale bars: 25 µm.

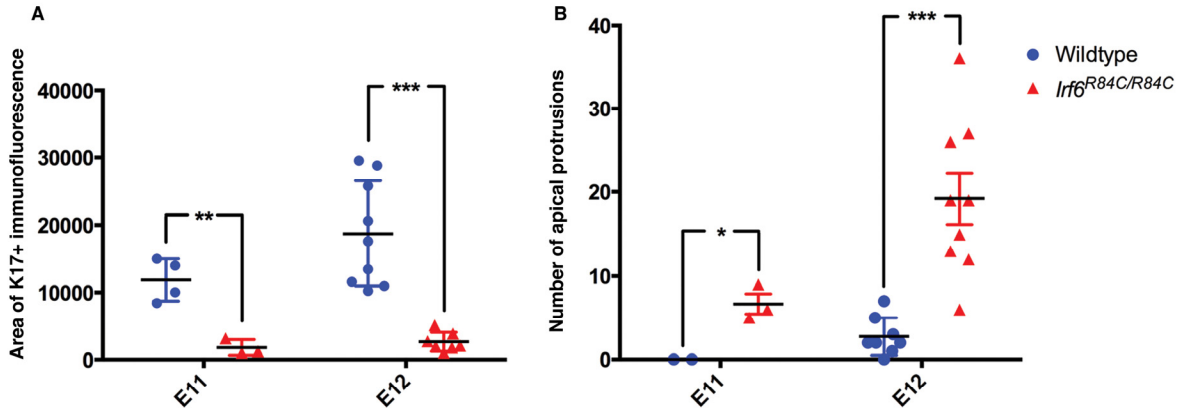

Supplemental Figure 4. Quantification of the area of K17 expression and number of apical protrusions in *Irf6*$^{R84C/R84C}$ mice and their wild-type littermates. (**A**) Dot plot showing quantification of the area of K17 immunofluorescence within a single field of view from wild-type (blue) and *Irf6*$^{R84C/R84C}$ (red) embryos at the ages indicated. The area of K17 staining was determined using ImageJ software. Wild-type: E11 – n=4, E12 – n=9; *Irf6*$^{R84C/R84C}$: E11 – n=2, E12 – n=7. (**B**) Dot plot demonstrating the number of apical protrusions observed in TEM images of wild-type (blue) or *Irf6*$^{R84C/R84C}$ embryos (red) at the ages indicated. Wild-type: E11 – n=2, E12 – n=8; *Irf6*$^{R84C/R84C}$: E11 – n=3, E12 – n=9. Analysis was performed on images from epidermis and oral epithelia from at least two different mice for each age and genotype. Statistical significance was calculated using a Student's t-test (* = $p < 0.05$; ** = $p < 0.01$; *** = $p < 0.001$).

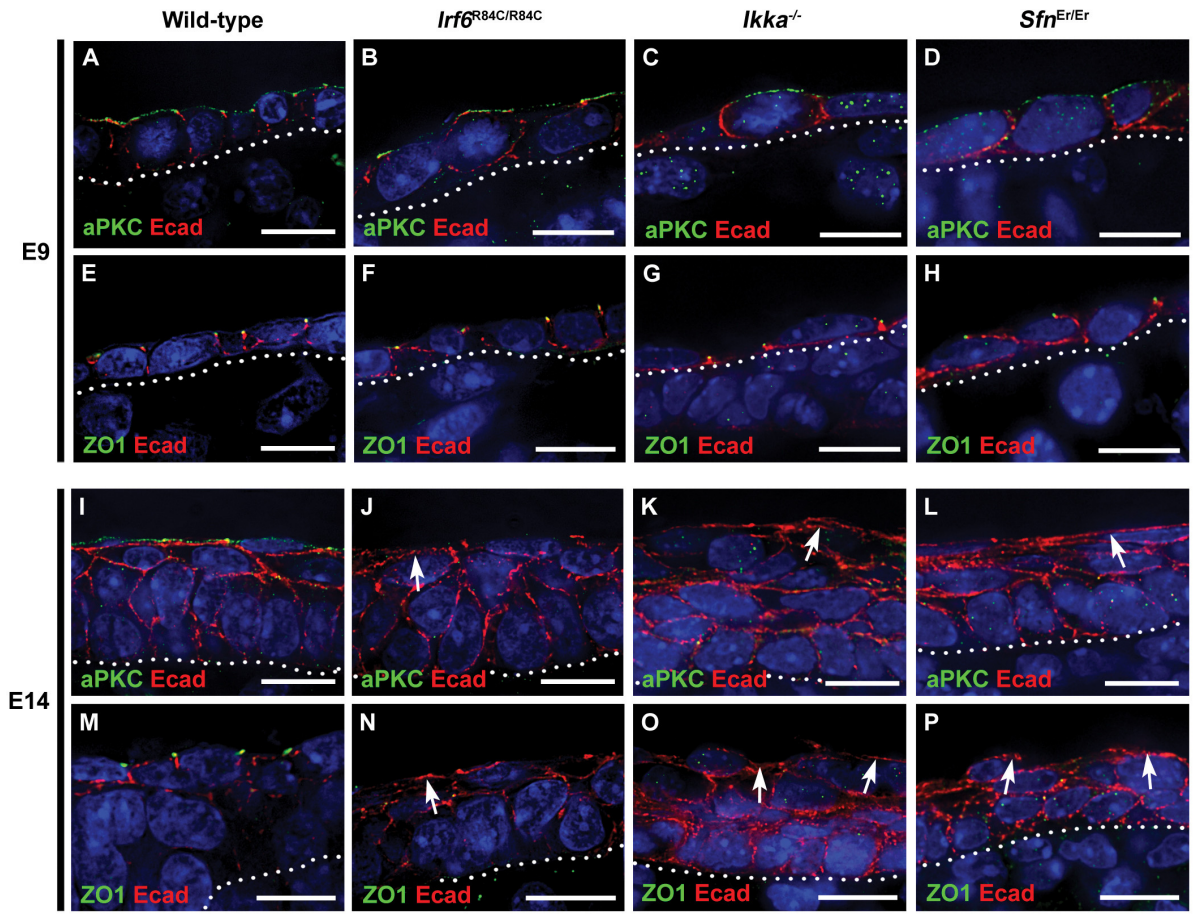

Supplemental Figure 5. Failure of periderm formation in *Irf6*$^{R84C/R84C}$, *Ikka*$^{-/-}$ and *Sfn*$^{Er/Er}$ mutant mice results in exposed adhesion complexes in developing epidermis. (**A-H**) At E9, prior to periderm formation, basal epithelial cells are highly polarized in wild-type and mutant mice. The polarity marker, atypical protein kinase C (aPKC) (**A-D**), and the tight junction component, ZO1 (**E-H**), are expressed apically in membranes and tight junctions of basal cells, respectively, whilst expression of E-cadherin is restricted to the adjacent membranes. (**I-M**) At E14, after periderm formation, expression of aPKC and ZO1 is highly polarized in the periderm of wild-type mice whilst E-cadherin is expressed in basal and intermediate cells but absent from the apical surface of periderm cells (**I** and **M**). However, in *Irf6*$^{R84C/R84C}$, *Ikka*$^{-/-}$ and *Sfn*$^{Er/Er}$ mutant mice where periderm formation is disrupted expression of aPKC and ZO1 are absent and E-cadherin is expressed on the apical membrane of exposed intermediate cells (**J-L** and **N-P**). Scale bars: 50 µm.

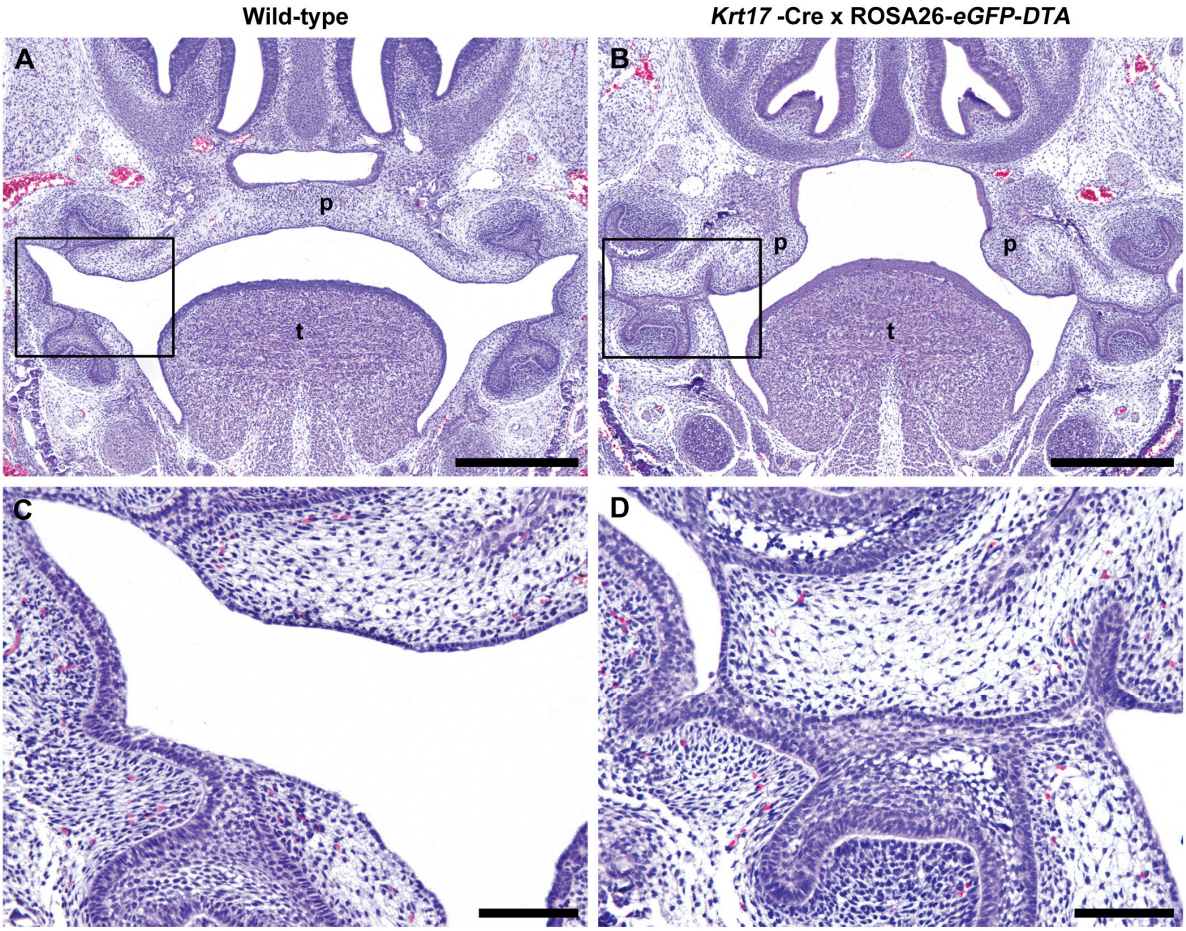

Supplemental Figure 6. Intra-oral epithelial adhesions following periderm ablation result in cleft palate in severe cases. (**A**) In E16 wild-type mice, in which the periderm forms normally, the palatal shelves have elevated above the tongue and fused in the midline. (**B**) In contrast, in *Krt17*-Cre x ROSA26-*eGFP-DTA* bi-transgenic mice, in which a subset of periderm cells are killed, inter-epithelial adhesions have formed between the maxillary and mandibular processes which have prevented complete elevation of the palatal shelves resulting in cleft palate. (**C** and **D**) Higher magnification images of the areas boxed in **A** and **B,** respectively, illustrate the inter-epithelial adhesions observed in *Krt17*-Cre x ROSA26-*eGFP-DTA* bi-transgenic mice. p, palatal shelf; t, tongue. Scale bars: **A** and **B**, 500 μm; **C** and **D**, 100 μm.

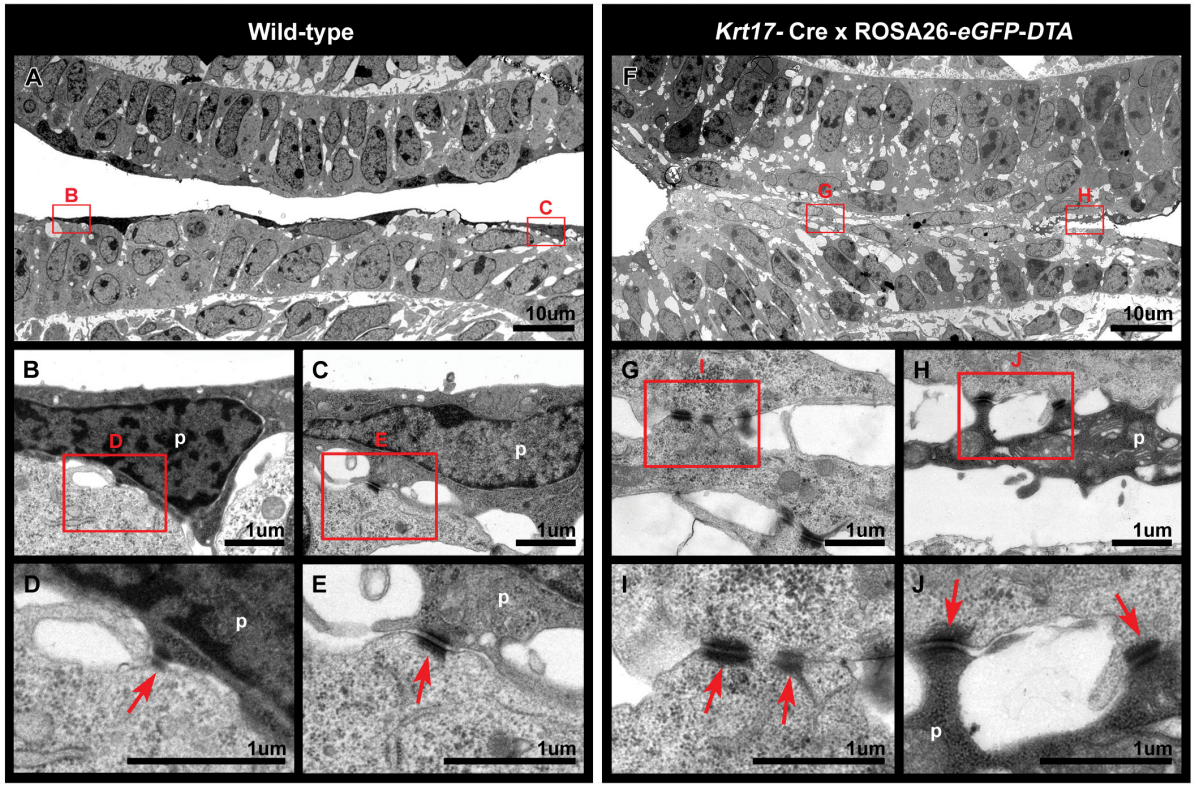

Supplemental Figure 7. *Krt17*-Cre x ROSA26-*eGFP-DTA* bi-transgenic mice lack electron-dense periderm within intra-oral fusions. (**A-E**) The oral epithelia of E13 wild-type mice are covered by a layer of electron-dense, flattened periderm cells (**A**). Within the periderm, desmosomes (arrows in **D** and **E**) are confined to the basal and lateral surfaces. (**F-J**) In *Krt17*-Cre x ROSA26-*eGFP-DTA* bi-transgenic mice, intra-oral adhesions have formed (**F**). In regions of inter-epithelial adhesions, the electron-dense periderm cells are absent and desmosomes form between the juxtaposed maxillary and mandibular epithelia (arrows in **I**). Where periderm cells have not been ablated, desmosomes do not form between the maxillary and mandibular epithelia and inter-epithelial adhesions are prevented. In these regions, desmosomes are confined to the basolateral surfaces of the periderm cells (arrows in **J**). p, periderm.